Fluvastatin prevents the development of arthritis in env-pX rats via up-regulation of Rho GTPase-activating protein 12

Short title: Effects of fluvastatin on rheumatoid arthritis

Shun Tanimura[1], Mutsumi Nishida[2], Tatsunori Horie[3], Tamotsu Kamishima[4], Hitomi Matsumoto[5], Yutaka Morimura[5], Yuka Nishibata[5], Sakiko Masuda[5], Daigo Nakazawa[1], Utano Tomaru[6], Tatsuya Atsumi[1], Akihiro Ishizu[5]

1) Department of Rheumatology, Endocrinology and Nephrology, Faculty of Medicine and Graduate School of Medicine, Hokkaido University, Sapporo, Japan.

2) Division of Laboratory and Transfusion Medicine, Hokkaido University Hospital, Sapporo, Japan.

3) Department of Radiological Technology, Hokkaido University Hospital, Sapporo, Japan.

4) Department of Biomedical Science and Engineering, Faculty of Health Sciences, Hokkaido University, Sapporo, Japan.

5) Department of Medical Laboratory Science, Faculty of Health Sciences, Hokkaido University, Sapporo, Japan.

6) Department of Pathology, Faculty of Medicine and Graduate School of Medicine, Hokkaido University, Sapporo, Japan.

Correspondence to:

Prof. Akihiro Ishizu, Faculty of Health Sciences, Hokkaido University, Kita-12, Nishi-5, Kita-ku, Sapporo 060-0812, Japan. E-mail: aishizu@med.hokudai.ac.jp

Abstract

The pleiotropic effects of statins, including an antiarthritic potential, have been noted. This study aimed to determine the efficacy of statins on rheumatoid arthritis (RA) and clarify how statins affect its pathogenesis. Fluvastatin (500 μg/kg/day) or vehicle was given per os to env-pX rats, which carry the human T-cell leukemia virus type I *env-pX* gene and spontaneously develop destructive arthritis mimicking RA, for 30 days. Blood sampling and ultrasonography (US) of the ankle joints were conducted on days 0, 10, 20, and 30. On day 30, all rats were euthanized, and the ankle joints were subjected to histological analysis. To clarify how fluvastatin affects the pathogenesis of RA, comprehensive serum exosomal microRNA (miRNA) analysis was performed. Gene expression in the primary culture of synovial fibroblasts derived from arthritic rat and human and non-arthritic rat periarticular tissues was determined quantitatively by real-time reverse transcription-polymerase chain reaction (RT-PCR). As a result, the development of arthritis in env-pX rats was significantly suppressed by fluvastatin, which was evident from the viewpoints of serology, US imaging, and histology. Comprehensive serum exosomal miRNA analysis suggested that the expression of *Rho GTPase-activating protein 12* (*Arhgap12*) was decreased in arthritic env-pX rats but increased with the administration of fluvastatin. Corresponding results were obtained by quantitative RT- PCR using primary culture of synovial fibroblasts. The collective findings suggest that fluvastatin prevents the development of arthritis in env-pX rats via the up-regulation of ARHGAP12. This study suggests that ARHGAP12 can be a possible therapeutic target of RA.

Key words: rheumatoid arthritis, fluvastatin, ARHGAP12

Abbreviations

Arhgap12, Rho GTPase-activating protein 12; GAP, GTPase-activating protein; Gapdh, glyceraldehyde 3-phosphate dehydrogenase; HMG-CoA, hydroxymethylglutaryl-coenzyme A; HTLV-I, human T-cell leukemia virus type I; IL, interleukin; miRNA, microRNA; MMP, matrix metalloproteinase; NF-κB, nuclear factor-κB; PD, power Doppler; RA, rheumatoid arthritis; RAPA, RA particle agglutination; RF, rheumatoid factor; Rho A, Ras homologous member A; ROI, region of interest; RT-PCR, reverse transcription-polymerase chain reaction; US, ultrasonography; WKAH, Wistar-King-Aptekman-Hokudai

1. Introduction

Rheumatoid arthritis (RA) is a common chronic inflammatory disease affecting approximately 0.5% to 1% of the world's population (McInnes and Schett, 2011) and characterized by the inflammatory cell infiltration of the synovium, cartilage degradation, and bone erosion. Inflammatory cytokines, particularly tumor necrosis factor-α, interleukin (IL)-17, and IL-1β, produced mainly by macrophages and T cells, are very important in the pathogenesis of RA, which activate matrix metalloproteinases (MMPs) and promote matrix catabolism and bone resorption (Miossec and Kolls, 2012). In addition, RA can be accompanied by the production of rheumatoid factor (RF) and anti-cyclic citrullinated peptide antibodies, the process of which is likely mediated by IL-21 (Burmester et al., 2014). Recently, several biological agents and compounds that can target molecules and cells involved in the pathogenesis of RA have revolutionized the management of RA (Wang et al., 2014). However, some of these drugs are still so expensive that not all patients can receive their therapeutic benefit and that their abuse can press the national medical finance. In addition, there are unavoidable adverse events, including opportunistic infection due to over-immunosuppression. Therefore, it is important to create more options for RA treatment that can be used safely and at a lower cost.

Statins, inhibitors of hydroxymethylglutaryl-coenzyme A (HMG-CoA) reductase, are the principal and reasonable therapeutic agents against hypercholesterolemia. HMG-CoA reductase is involved in the first step committed in sterol biosynthesis in hepatocytes and the key enzyme that converts HMG-CoA into mevalonate, a cholesterol precursor. Recently, the pleiotropic effects of statins have been noted (Bedi et al., 2016; Liao and Laufs, 2005). By inhibiting L-mevalonic acid synthesis, statins can also prevent the synthesis of other isoprenoid intermediates of the cholesterol biosynthetic pathway, such as farnesyl pyrophosphate and geranylgeranyl

pyrophosphate (Goldstein and Brown, 1990). These intermediates serve as lipid attachments for the post- translational modification of a variety of proteins, including the γ-subunit of heterotrimeric G proteins, heme A, nuclear lamins, small GTP-binding protein Ras, and Ras-like proteins, such as Rho, Rab, Rac, Ral, and Rap (Van Aelst and D'Souza-Schorey, 1997). These proteins possess diverse functions and are involved in various disorders, including cardiorenal syndrome, atherosclerosis, diabetic complications, and dementia (Deakin et al., 2003; Li et al., 2005; Mahajan and Dhawan, 2010; Reiss and Wirkowski, 2007; Vaughan, 2003; Yagi et al., 2008). Thus, expectedly, statins can also mediate cholesterol-unrelated effects, such as anti-inflammatory, antiproliferative, antioxidant, immunomodulatory, and antithrombotic effects (DuBroff and de Lorgeril, 2015) without immunosuppression. In addition, some cohort studies have suggested the benefits of statin use in RA patients (Chodick et al., 2010; Das et al., 2015; McCarey et al., 2004). However, it remains to be revealed how statins affect the pathogenesis of RA.

The aim of this study was to determine the therapeutic efficacy of statins on RA and how they affect its pathogenesis. For this purpose, env-pX rats, which carry the *env-pX* gene of human T-cell leukemia virus type I (HTLV-I) in the germline of Wistar-King-Aptekman-Hokudai (WKAH) rats under the control of the HTLV-I long terminal repeat promoter (Yamazaki et al., 1997), were employed. The *env-pX* transgene was expressed ubiquitously in systemic organs, including synovial cells. Because the transgene coded the transcription factor p40tax, which could disturb the ordinary transcription in the cells, but did not code other viral constructive proteins, these rats were considered as models of abnormal gene transcription rather than simple models of HTLV-I infection (Ishizu and Yoshiki, 2012). env-pX rats are unique models that spontaneously develop progressive arthritis consequent on the molecular disturbance in synovial cells. The similarity of this pathogenesis to that of human RA was the reason why this model was employed in the present study.

2. Materials and Methods

2.1. Rats and cells

env-pX rats (Yamazaki et al., 1997) and wild-type WKAH rats were used. These rats were maintained at the Institute for Animal Experimentation, Hokkaido University Graduate School of Medicine. Primary culture cells of synovial fibroblasts obtained from an arthritic env-pX rat (TJF-1) and a non-arthritic WKAH rat (NF-1; Ishizu et al., 2003) were used. Experiments using rats were performed in accordance with the Guidelines for the Care and Use of Laboratory Animals in Hokkaido University.

Primary culture cells of synovial fibroblasts obtained from a patient with RA (FLS; Kono et al., 2015) were also used. The protocol for the collection and use of human synovial materials was approved by the institutional review board of Hokkaido University Hospital (Permission No. 008-0103).

2.2. Reagents

Fluvastatin was purchased from Fujifilm Wako Pure Chemical (Osaka, Japan). Dextrose grape sugar was purchased from Nacalai Tesque (Kyoto, Japan). The assay kit of serum RA particle agglutination (RAPA) was purchased from Fujirebio (Tokyo, Japan).

2.3. Study design

Male env-pX rats (8 weeks old; n=11) were divided into two groups. At the beginning of this study, all rats did not show joint swelling. In Group 1 (fluvastatin group), fluvastatin (500 μg/kg/day) was given per os to env-pX rats (n=6) for 30 days. The dose was comparable to the upper limit in human medication. In Group 2 (control group), vehicle

solution (5% glucose) was given similarly to env-pX rats (n=5).

The condition of rats was observed every day. On days 0, 10, 20, and 30, peripheral blood was obtained by tail cut, and the longitudinal view of the bilateral ankle joints was obtained by ultrasonography (US) with power Doppler (PD). On day 30, all rats were euthanized, and the ankle joints were subjected to histological analysis. This study was approved by the Animal Experiment Committee of Hokkaido University (Permission No. 10-0029, 15-0034).

2.4. Joint US

env-pX rats were sedated under inhalation anesthesia, and then the bilateral ankle joints were scanned with longitudinal view by US in the state of lateral decubitus position. All env-pX rats were examined by either of two sonographers with 8 or 32 years of experience in clinical US. The US equipment used was Logiq e Premium (GE Healthcare, Tokyo, Japan) with L10-22 RS probe. At first, the ankle joint was visualized by identifying the tibia and the metatarsal bone in grayscale images; thereafter, a sweep scan was performed by covering the whole ankle joint by PD. The PD gain was set to the maximum value of the discrepancy in which the noise disappeared. When the region with the strongest blood flow signaling was detected by PD, the findings were captured as still images. The PD values were determined as the pixels counted in manually defined region of interests (ROIs) using ImageJ 1.50i software (http://allpcworld.com/download-imagej-1-50i-free/).

2.5. Histological scores of arthritis

The resected ankle joints were fixed with 10% formalin and then decalcified in 10% ethylenediaminetetraacetic acid-disodium salt solution. Several weeks later, the joint tissues with a sagittal dissection were embedded in paraffin. The formalin-fixed

paraffin-embedded tissues were cut into 4 μm sections, deparaffinized with xylene, and then subjected to hematoxylin and eosin staining.

Histological analysis was done using the 0 to 3 grading system (0, normal; 1, mild; 2, moderate; 3, severe) concerning three different histological features of RA (Williams et al., 1992): periarticular inflammation (infiltration of mononuclear cells), synovial hypertrophy (pannus formation), and subchondral bone erosion. Scoring was done by a board certified member of the Japanese Society of Pathology with 16 years of experience. The total score was determined as the sum of the scores for the three parameters.

2.6. Comprehensive serum exosomal micro RNA (miRNA) analysis

Comprehensive serum exosomal miRNA analysis was performed using serum samples obtained from Group 1 (fluvastatin-treated) and Group 2 (untreated) env-pX rats on day 30 and from age- and gender-matched wild-type WKAH rats as controls (Toray Industries, Tokyo, Japan). In brief, RNAs were extracted from the sera using 3D-gene RNA extraction reagent from liquid sample kit followed by fluorescence labeling. These samples, as probes, were next applied to rat miRNA Oligo Chip equipped with 761 miRNAs. To avoid the detection of individual differences in miRNA expression, three randomly chosen samples from each group were mixed and subjected to assay.

2.7. Real-time reverse transcriptase-polymerase chain reaction (RT-PCR)

Total RNA was isolated from the rat and human primary culture cells of synovial fibroblasts (TJF-1, NF-1, and FLS) using the RNeasy Plus Mini kit (Qiagen, Hulsterweg, The Netherlands) and then converted into complementary DNA using a SuperScript VILO cDNA Synthesis kit (Life Technologies, Tokyo, Japan). Real-time RT-PCR was

performed to examine the mRNA expression levels of *Rho GTPase-activating protein 12* (*Arhgap12*) and *glyceraldehyde 3-phosphate dehydrogenase* (*Gapdh*) as internal reference in the cells using an Applied Biosystems 7500 Fast Real-Time PCR System (Foster City, CA, USA) with TaqMan MGB probes or LightCycler 480 (Roche, Basel, Switzerland) with Fast SYBR Green Master Mix. PCR was carried out as follows: initial denaturation at 95°C for 5 min followed by 40 cycles of denaturation at 95°C for 15 s, annealing at 60°C for 15 s, and extension at 72°C for 30 s. The primer sequences are shown in **Table S1**. The mRNA expression levels were quantified by the ΔΔCT method.

2.8. Statistical analysis

Kaplan-Meier comparison between groups was assessed using the log-rank test. Student's *t*-test was employed to compare the differences between two parametric groups. All analyses were performed using the JMP Pro software (version 12.0; SAS Institute, Cary, NC, USA) and GraphPad Prism software (version 7.02; GraphPad Software, San Diego, CA, USA).

3. Results

3.1. Effect of fluvastatin on joint swelling

Male env-pX rats (8 weeks old) administered with or without fluvastatin (500 μg/kg/day) were monitored for 30 days. The chronological progression of joint swelling of the legs is shown in **Figure 1**. The rates of the lower legs with joint swelling were significantly lower in Group 1 (fluvastatin group, n=6; total joint count, n=12) compared to Group 2 (control group, n=5; total joint count, n=10) after day 18 ($p<0.01$).

3.2. Effect of fluvastatin on RF

Repeated sampling of blood every 10 days was succeeded in five rats in Group 1 (fluvastatin group) and four rats in Group 2 (control group). Concerning these samples, RF was determined as a RAPA titer (**Table 1**). On day 30, RF was positive in one of the five rats in Group 1 (fluvastatin group), whereas three of the four rats exhibited positivity for RF in Group 2 (control group).

3.3. Effect of fluvastatin on US findings

The representative macroscopic and US findings of the rat ankle joints with and without swelling are shown in **Figure S1**. Using the images obtained by grayscale US, the ROI that displays the synovium was determined manually and then the thickness of the synovium was measured. The PD values were determined as the pixels counted in manually defined ROIs using ImageJ software. Based on the data obtained every 10 days in this way, the chronological thickening of the synovium and the increase in PD values are shown in **Figure 2**. US revealed that synovial thickening tended to be suppressed in Group 1 (fluvastatin group) compared to Group 2 (control group), although the difference

was not statistically significant (**Figure 2a**; p=0.117). It is notable that the increase in PD values was significantly inhibited by fluvastatin (**Figure 2b**; on day 30, Group 1 versus Group 2, p=0.028). The representative change of PD images in Group 1 (fluvastatin-treated) and Group 2 (control) rats is shown in **Figures 2c** and **2d**, respectively.

3.4. Effect of fluvastatin on histological findings

The histological scores of RA according to the grade of periarticular inflammation (infiltration of mononuclear cells), synovial hypertrophy (pannus formation), and subchondral bone erosion were determined (**Figure S2**). The total histological scores and the scores in each parameter in Group 1 (fluvastatin group) were significantly lower than those in Group 2 (control group; **Figure 3**).

3.5. Comprehensive serum exosomal miRNA analysis

To clarify how fluvastatin affected the pathogenesis of RA, comprehensive serum exosomal miRNA analysis was performed using serum samples obtained from Group 1 (fluvastatin-treated) and Group 2 (untreated) env-pX rats on day 30 and from wild-type WKAH rats as reference. Among miRNAs detected in the serum samples of Groups 1 and 2 rats (**Figure 4a**), those that exhibited more than twice the difference in the expression level between the groups are listed in **Table S2**. Interestingly, rno-miR-17-5p, rno-miR-20a-5p, and rno-miR-20b-5p were similarly decreased in Group 1 (fluvastatin-treated env-pX rats), whereas they all were increased in Group 2 (non-treated env-pX rats) compared to the non-arthritic wild-type controls (**Figure 4b**). In addition, these miRNAs could target the same gene, *Arhgap12* (**Table S2**).

3.6. mRNA expression level of Arhgap12 was decreased in arthritic synovial

fibroblasts and increased by fluvastatin

The expression levels of *Arhgap12* in the primary culture of synovial fibroblasts, NF-1 (derived from a non-arthritic WKAH rat) and TJF-1 (derived from an arthritic env-pX rat), were determined by real-time RT-PCR (**Figure 5a**). The expression was significantly lower in TJF-1 than in NF-1 ($p<0.001$). Next, the alteration of *Arhgap12* mRNA expression induced by fluvastatin (1 μM) by real-time RT-PCR was determined (**Figure 5b**). Results demonstrated that the *Arhgap12* mRNA expression level was significantly increased by fluvastatin (1 μM) in TJF-1 ($p=0.034$), whereas no significant alteration was seen in NF-1. Correspondingly, the *Arhgap12* mRNA expression level was significantly increased by fluvastatin (1 μM) in FLS derived from synovial tissues of a patient with RA (**Figure 5c**; $p<0.001$).

4. Discussion

In the trial of atorvastatin in RA (a 6-month period, placebo-controlled, and randomized clinical trial with atorvastatin), the additional treatment with atorvastatin was suggested to reduce RA activity (p=0.004), swollen joint scores (p=0.006), and serum C-reactive protein levels (p<0.001; McCarey et al., 2004). Moreover, other reports also supported the opposite correlation between statin use and RA risk (Chodick et al., 2010; Das et al., 2015). However, there is a report demonstrating that statin has no apparent effect on RA activity (Akiyama et al., 2015). Therefore, the inhibitory effect of statins on arthritis remains controversial. Ahmed et al. (2015) examined the antiarthritic effects of simvastatin on complete Freund's adjuvant-induced RA in rats and demonstrated that simvastatin significantly restored the levels of biomarkers, such as MMP-3, cartilage oligomeric matrix protein, and glutathione, to normal limits. Barbosa et al. (2014) also demonstrated the protective effect of simvastatin on the histopathological destruction of joints induced by complete Freund's adjuvant in rats.

To determine whether statins could contribute to RA clinic, env-pX rats that mimic the autoimmune pathogenesis of human RA (Ishizu and Yoshiki, 2012; Yamazaki et al., 1997) were employed. In these rats, chronic destructive arthritis spontaneously developed with a production of high titers of RF. The present study clearly demonstrated the inhibitory effect of fluvastatin on arthritis that developed in env-pX rats from the viewpoints of serology, US imaging, and histology. To monitor the progression of synovitis chronologically, joint US was used in this study. Up to now, there are few studies that use US to evaluate arthritis in small animals (Clavel et al., 2008; Horie et al., 2019; Liao et al., 2016). The recent development of US makes it possible to image more clearly using higher frequencies without motion artifacts. The results presented in this study suggested that joint US could evaluate the progression of synovitis acurately even in small animals.

As hyperlipidemia has not been noted as a risk of RA development, it was suspected that the effects of fluvastatin, other than the reduction of the serum cholesterol level, could contribute to the suppression of the development of arthritis in env-pX rats. To clarify how fluvastatin suppressed the development of arthritis in env-pX rats, comprehensive serum exosomal miRNA analysis was carried out, and the expression levels of rno-miR-17-5p, rno-miR-20a-5p, and rno-miR-20b-5p were found to be decreased by fluvastatin treatment, whereas these levels were increased in non-treated arthritic env-pX rats compared to non-arthritic wild-type rats. The common target gene of these miRNAs is *Arhgap12*. Because miRNAs negatively regulate the expression of the target gene, this result speculated that the expression level of *Arhgap12* may be decreased in arthritic env-pX rats and increased by fluvastatin treatment. Quantitative RT-PCR using cultured synovial fibroblasts derived from an arthritic env-pX rat (TJF-1) and a non-arthritic wild-type rat (NF-1) demonstrated that *Arhgap12* mRNA expression was significantly lower in TJF-1 than in NF-1 and was significantly increased by fluvastatin in TJF-1 but not in NF-1. Moreover, similar results were reproduced when human arthritic synovial fibroblasts FLS were used for the same assay. These findings suggested that the dynamics of serum miRNAs was reflected in the altered gene expression in synovial tissues at least in part.

Rho GTPases constitute a subfamily of the Ras superfamily of small GTPases, such as Ras homologous member A (RhoA), Ras-related C3 botulinum toxin substrate 1, and cell division cycle 42. They exist in two forms, namely, a GDP-bound inactive form and a GTP-bound active form. Guanine nucleotide exchange factors facilitate the exchange of GDP for GTP, thereby transforming Rho GTPases from the inactive form to the active form. The activated Rho GTPases can bind to various effectors, including Rho kinases, and elicit diverse biological activities. In contrast, GTPase-activating proteins (GAPs) increase the endogenous GTPase activity of Rho GTPases via hydrolysis of GTP on Rho, resulting in a promoted transformation of Rho GTPases from the active

form to the inactive form (Luo, 2000). ARHGAP12 is one of the GAPs.

There are some reports suggesting the mechanisms of how statins inhibit the pathogenesis of RA. The activation of Rho kinases induced nuclear factor-κB (NF-κB) activation and the subsequent production of pro-inflammatory cytokines in RA synoviocytes (see schematic cartoon in **Figure 5d**), and simvastatin and other Rho kinase blockades inhibited NF-κB activation, resulting in the amelioration of the RA phenotype (He et al., 2008; Xu et al., 2006). Thus, it was hypothethized that fluvastatin can up-regulate ARHGAP12 in synovial tissues, resulting in the transformation of Rho GTPases from the active form to the inactive form, settling down Rho kinase and NF-κB activities, and suppression of artiritis in env-pX rats. Further studies are needed to elucidate this hypothesis. Other mechanisms should be also considered as fluvastatin was reported to induce apoptosis in RA synoviocytes through the mitochondria- and caspase 3-dependent pathways (Nagashima et al., 2006; Nanke et al., 2009).

T cells from RA-prone mice exhibited excessive Rho kinase activation, and Rho kinase inhibitors decreased the production of IL-17 and IL-21 from T cells *in vitro* (Biswas et al., 2010). *Arhgap12* gene has a wide spectrum of expression profile, is also expressed in hematopoietic cells, such as macrophages and neutrophilic granulocytes, and is involved in the regulation of phagocytosis (Schlam et al., 2015). Therefore, an investigation into the roles of ARHGAP12 in hematopoietic immune cells and their contribution to the pathogenesis of RA are important future subjects.

In this study, the efficacy of fluvastatin was examined only in a single dose (500 μg/kg/day). Although this is within the human medication dose, the dose-dependent efficacy of fluvastatin remains undetermined. In addition, the efficacy of statins other than fluvastatin was not determined. These limitations will be the subjects of further studies. Despite these limitations, this study suggests that fluvastatin has antiarthritic and immunomodulatory potential and that statins, including fluvastatin, can be a new

supportive drug for RA. Furthermore, putative reagents that up-regulate ARHGAP12 as well as fluvastatin can be candidates for RA curatives.

Acknowledgements

The authors are very grateful to the staff of Hokkaido University and Hokkaido University Hospital for husbandry and advice.

Conflict of interests

Tatsuya Atsumi received grant/research support from Takeda Pharmaceutical Co., Ltd., Chugai Pharmaceutical Co., Ltd., AbbVie, Inc., Daiichi Sankyo Co., Ltd., Astellas Pharma, Inc., AYUMI Pharmaceutical Corp., Asahi Kasei Pharma Corporation, Eisai Co., Ltd., and Mitsubishi Tanabe Pharma Co. and has taken part in speakers' bureaus for Takeda Pharmaceutical Co., Ltd., Chugai Pharmaceutical Co., Ltd., AbbVie, Inc., Bristol-Myers Squibb Co., Daiichi Sankyo Co., Ltd., Astellas Pharma, Inc., AYUMI Pharmaceutical Corp., UCB Japan Co., Ltd., Novartis Co., Janssen Pharmaceutical K.K., Asahi Kasei Pharma Corporation, Eisai Co., Ltd., Alexion, Inc., and Mitsubishi Tanabe Pharma Co. The other authors declare that they have no conflict of interest.

References

Ahmed, Y. M., Messiha, B. A., Abo-Saif, A. A., 2015. Protective Effects of Simvastatin and Hesperidin against Complete Freund's Adjuvant-Induced Rheumatoid Arthritis in Rats. Pharmacology 96, 217-225.

Akiyama, M., Mawatari, T., Nakashima, Y., Miyahara, H., Yamada, H., et al., 2015. Prevalence of dyslipidemia in Japanese patients with rheumatoid arthritis and effects of atorvastatin treatment. Clin Rheumatol. 34, 1867-1875.

Barbosa, C. P., Ritter, A. M., da Silva, L. G., Grespan, R., Cuman, R. K., et al., 2014. Effects of simvastatin, ezetimibe, and their combination on histopathologic alterations caused by adjuvant-induced arthritis. Inflammation. 37, 1035-1043.

Bedi, O., Dhawan, V., Sharma, P. L., Kumar, P., 2016. Pleiotropic effects of statins: new therapeutic targets in drug design. Naunyn Schmiedebergs Arch Pharmacol. 389, 695-712.

Biswas, P. S., Gupta, S., Chang, E., Song, L., Stirzaker, R.A., et al., 2010. Phosphorylation of IRF4 by ROCK2 regulates IL-17 and IL-21 production and the development of autoimmunity in mice. J Clin Invest. 120, 3280-3295.

Burmester, G. R., Feist, E., Dorner, T., 2014. Emerging cell and cytokine targets in rheumatoid arthritis. Nat Rev Rheumatol. 10, 77-88.

Chodick, G., Amital, H., Shalem, Y., Kokia, E., Heymann, A. D., et al., 2010. Persistence with statins and onset of rheumatoid arthritis: a population-based cohort study. PLoS Med. 7, e1000336.

Clavel. G., Marchiol-Fournigault, C., Renault, G., Boissier, M. C., Fradelizi, D., et al., 2008. Ultrasound and Doppler micro-imaging in a model of rheumatoid arthritis in mice. Ann Rheum Dis. 67, 1765-1772.

Das, S., Mohanty, M., Padhan, P., 2015. Outcome of rheumatoid arthritis following adjunct statin therapy. Indian J Pharmacol. 47, 605-609.

Deakin, S., Leviev, I., Guernier, S., James, R. W., 2003. Simvastatin modulates expression of the PON1 gene and increases serum paraoxonase: a role for sterol regulatory element-binding protein-2. Arterioscler Thromb Vasc Biol. 23, 2083-2089.
DuBroff, R., de Lorgeril, M., 2015. Cholesterol confusion and statin controversy. World J Cardiol. 7, 404-409.

Goldstein, J. L., Brown, M. S., 1990. Regulation of the mevalonate pathway. Nature. 343, 425-430.

He, Y., Xu, H., Liang, L., Zhan, Z., Yang, X., et al., 2008. Antiinflammatory effect of Rho kinase blockade via inhibition of NF-κB activation in rheumatoid arthritis. Arthritis Rheum. 58, 3366-3376.

Horie, T., Nishida, M., Tanimura, S., Kamishima, T., Tamai, E., et al., 2019. Detection of Increased Vascular Signal in Arthritis-Prone Rats Without Joint Swelling Using Superb Microvascular Imaging Ultrasonography. Ultrasound Med Biol. 45, 2086-2093.

Ishizu, A., Tsuji, T., Abe, A., Saito, S., Takahashi, T., et al., 2003. Transduction of dominant negative ATF-1 suppresses the pX gene expression in joint fibroblastic cells derived from HTLV-I transgenic rats. Exp Mol Pathol. 74, 309-313.

Ishizu, A., Yoshiki, T., 2012. Pathogenesis of Vasculitis in env-pX Rats. Ann Vasc Dis.5, 296-299.

Kono, M., Yasuda, S., Stevens, R. L., Koide, H., Kurita, T., et al., 2015. Ras Guanine Nucleotide-Releasing Protein 4 Is Aberrantly Expressed in the Fibroblast-Like Synoviocytes of Patients With Rheumatoid Arthritis and Controls Their Proliferation. Arthritis Rheumatol 67, 396-407.

Li, F., Drel, V. R., Szabo, C., Stevens, M. J., Obrosova, I. G., 2005. Low-dose poly(ADP-ribose) polymerase inhibitor-containing combination therapies reverse early peripheral

diabetic neuropathy. Diabetes. 54, 1514-1522.

Liao, A. H., Chung, H. Y., Chen, W. S., Yeh, M. K., 2016. Efficacy of Combined Ultrasound-and-Microbubbles-Mediated Diclofenac Gel Delivery to Enhance Transdermal Permeation in Adjuvant-Induced Rheumatoid Arthritis in the Rat. Ultrasound Med Biol. 42, 1976-1985.

Liao, J. K., Laufs, U., 2005. Pleiotropic effects of statins. Annu Rev Pharmacol Toxicol. 45, 89-118.

Luo, L., 2000. Rho GTPases in neuronal morphogenesis. Nat Rev Neurosci. 1, 173-180.

Mahajan, N., Dhawan, V., 2010. In vitro modulation of peroxisome proliferator-activated receptor-gamma and its genes by C-reactive protein. Role of atorvastatin. Arch Med Res. 41, 154-161.

McCarey, D. W., McInnes, I. B., Madhok, R., Hampson, R., Scherbakov, O., et al., 2004. Trial of Atorvastatin in Rheumatoid Arthritis (TARA): double-blind, randomised placebo-controlled trial. Lancet. 363, 2015-2021.

McInnes, I. B., Schett, G., 2011. The pathogenesis of rheumatoid arthritis. N Engl J Med. 365, 2205-2219.

Miossec, P., Kolls, J. K., 2012. Targeting IL-17 and TH17 cells in chronic inflammation. Nat Rev Drug Discov. 11, 763-776.

Nagashima, T., Okazaki, H., Yudoh, K., Matsuno, H., Minota, S., 2006. Apoptosis of rheumatoid synovial cells by statins through the blocking of protein geranylgeranylation: a potential therapeutic approach to rheumatoid arthritis. Arthritis Rheum. 54, 579-586.

Nanke, Y., Kawamoto, M., Yago, T., Chiba, J., Yamanaka, H., et al., 2009. Geranylgeranylacetone, a non-toxic inducer of heat shock protein, induces cell death

in fibroblast-like synoviocytes from patients with rheumatoid arthritis. Mod Rheumatol. 19, 379-383.

Reiss, A. B., Wirkowski, E., 2007. Role of HMG-CoA reductase inhibitors in neurological disorders : progress to date. Drugs. 67, 2111-2120.

Schlam, D., Bagshaw, R. D., Freeman, S. A., Collins, R. F., Pawson, T., et al., 2015. Phosphoinositide 3-kinase enables phagocytosis of large particles by terminating actin assembly through Rac/Cdc42 GTPase-activating proteins. Nat Commun. 6, 8623.

Van Aelst, L., D'Souza-Schorey, C., 1997. Rho GTPases and signaling networks. Genes Dev. 11, 2295-2322.

Vaughan, C. J., 2003. Prevention of stroke and dementia with statins: Effects beyond lipid lowering. Am J Cardiol. 91, 23b-29b.

Wang, D., Li, Y., Liu, Y., Shi, G., 2014. The use of biologic therapies in the treatment of rheumatoid arthritis. Curr Pharm Biotechnol. 15, 542-548.

Williams, R. O., Feldmann, M., Maini, R. N., 1992. Anti-tumor necrosis factor ameliorates joint disease in murine collagen-induced arthritis. Proc Natl Acad Sci USA. 89, 9784-9788.

Xu, H., Liu, P., Liang, L., Danesh, F. R., Yang, X., et al., 2006. RhoA-mediated, tumor necrosis factor α-induced activation of NF-κB in rheumatoid synoviocytes: inhibitory effect of simvastatin. Arthritis Rheum. 54, 3441-3451.

Yagi, S., Aihara, K., Ikeda, Y., Sumitomo, Y., Yoshida, S., et al., 2008. Pitavastatin, an HMG-CoA reductase inhibitor, exerts eNOS-independent protective actions against angiotensin II induced cardiovascular remodeling and renal insufficiency. Circ Res. 102, 68-76.

Yamazaki, H., Ikeda, H., Ishizu, A., Nakamaru, Y., Sugaya, T., et al., 1997. A wide spectrum of collagen vascular and autoimmune diseases in transgenic rats carrying the env-pX gene of human T lymphocyte virus type I. Int Immunol. 9, 339-346.

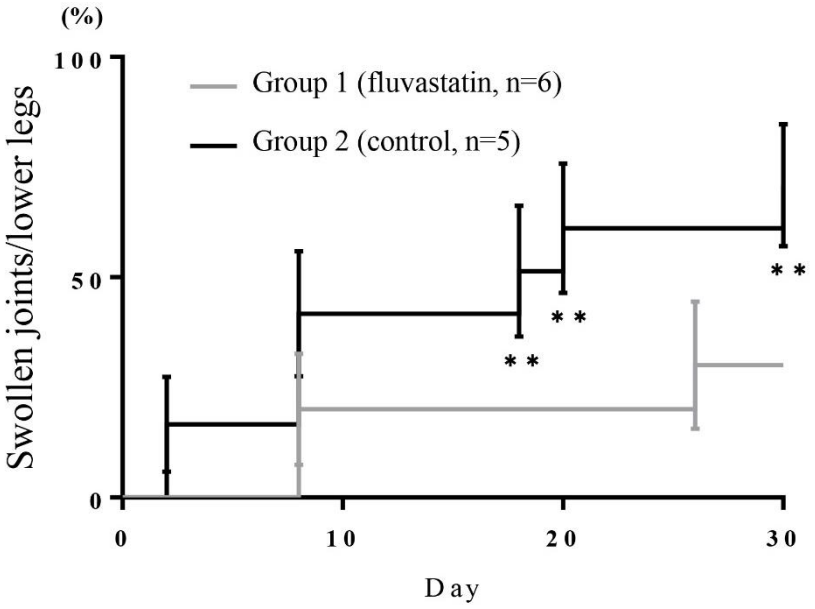

Figure 1. Effect of fluvastatin on joint swelling

The chronological change of the rates of the lower legs with joint swelling is shown. ***p*<0.01 (Kaplan-Meier log-rank test).

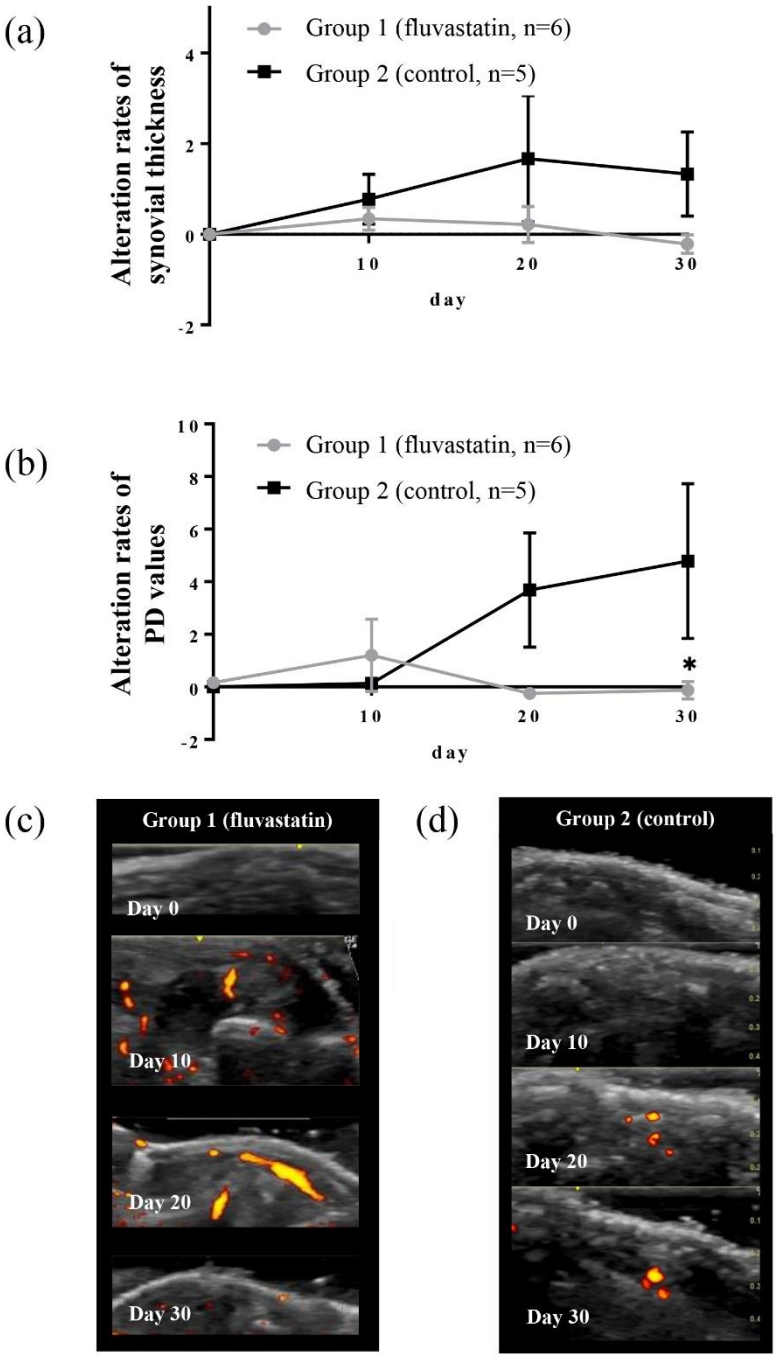

Figure 2. Effect of fluvastatin on US findings

(**a**) Chronological alteration rates of synovial thickness. (**b**) Chronological alteration rates of PD values. Data are mean±standard error (SE). **p*<0.05 (Student's *t*-test). (**c and d**) Representative change of PD images in Group 1 (fluvastatin-treated; **c**) and Group 2 (control; **d**) rats. PD images on days 0, 10, 20, and 30 obtained from the same rat in each group are shown.

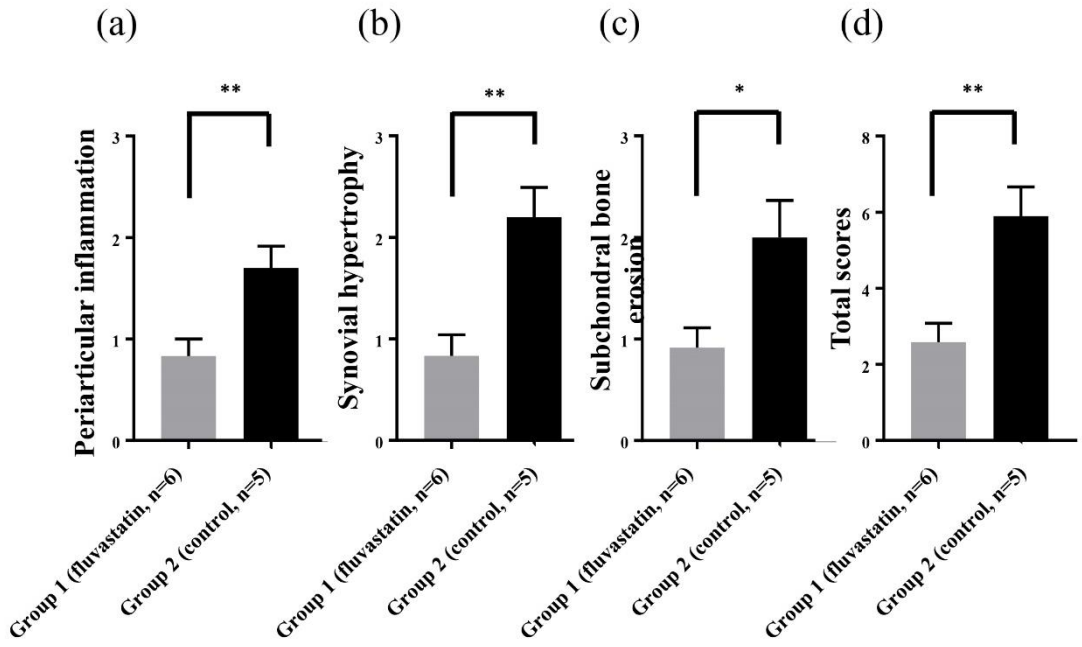

Figure 3. Effect of fluvastatin on histological findings

Comparison of histological scores of periarticular inflammation (infiltration of mononuclear cells; **a**), synovial hypertrophy (pannus formation; **b**), and subchondral bone erosion (**c**) and total scores (**d**) between Group 1 (fluvastatin group) and Group 2 (control group). Data are mean±SE. **p*<0.05, ***p*<0.01 (Student's *t*-test).

(a)

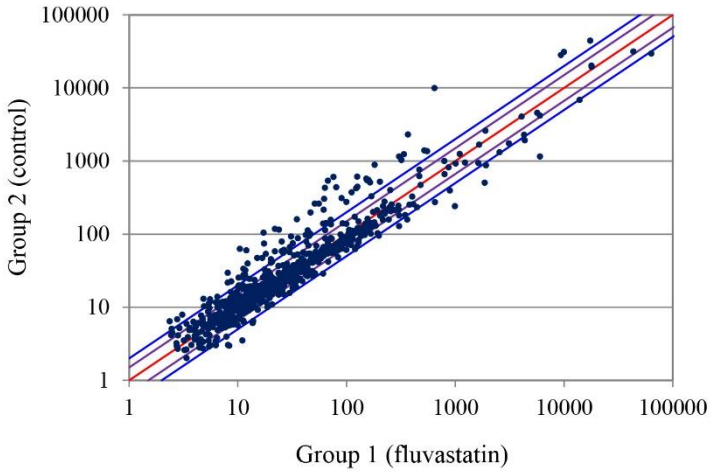

(b)

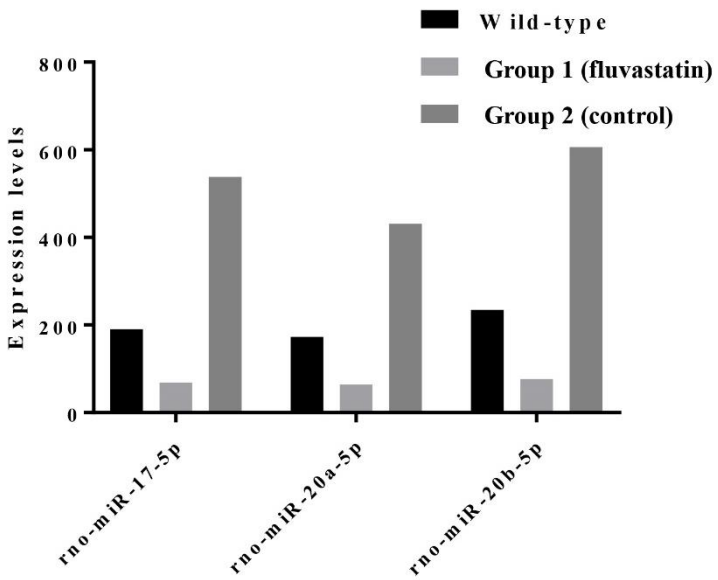

miRNA	Group 2/Group 1 Ratio
rno-miR-17-5p	7.96
rno-miR-20a-5p	7.95
rno-miR-20b-5p	6.79

Figure 4. Comprehensive serum exosomal miRNA analysis

(**a**) Comparison of the expression levels of whole miRNAs between Groups 1 and 2. (**b**) Expression levels of rno-miR-17-5p, rno-miR-20a-5p, and rno-miR-20b-5p among wild-type rats, Group 1 (fluvastatin-treated env-pX) rats, and Group 2 (non-treated env-pX) rats. The expression ratios of rno-miR-17-5p, rno-miR-20a-5p, and rno-miR-20b-5p (Group 2/Group 1) are shown in the bottom table.

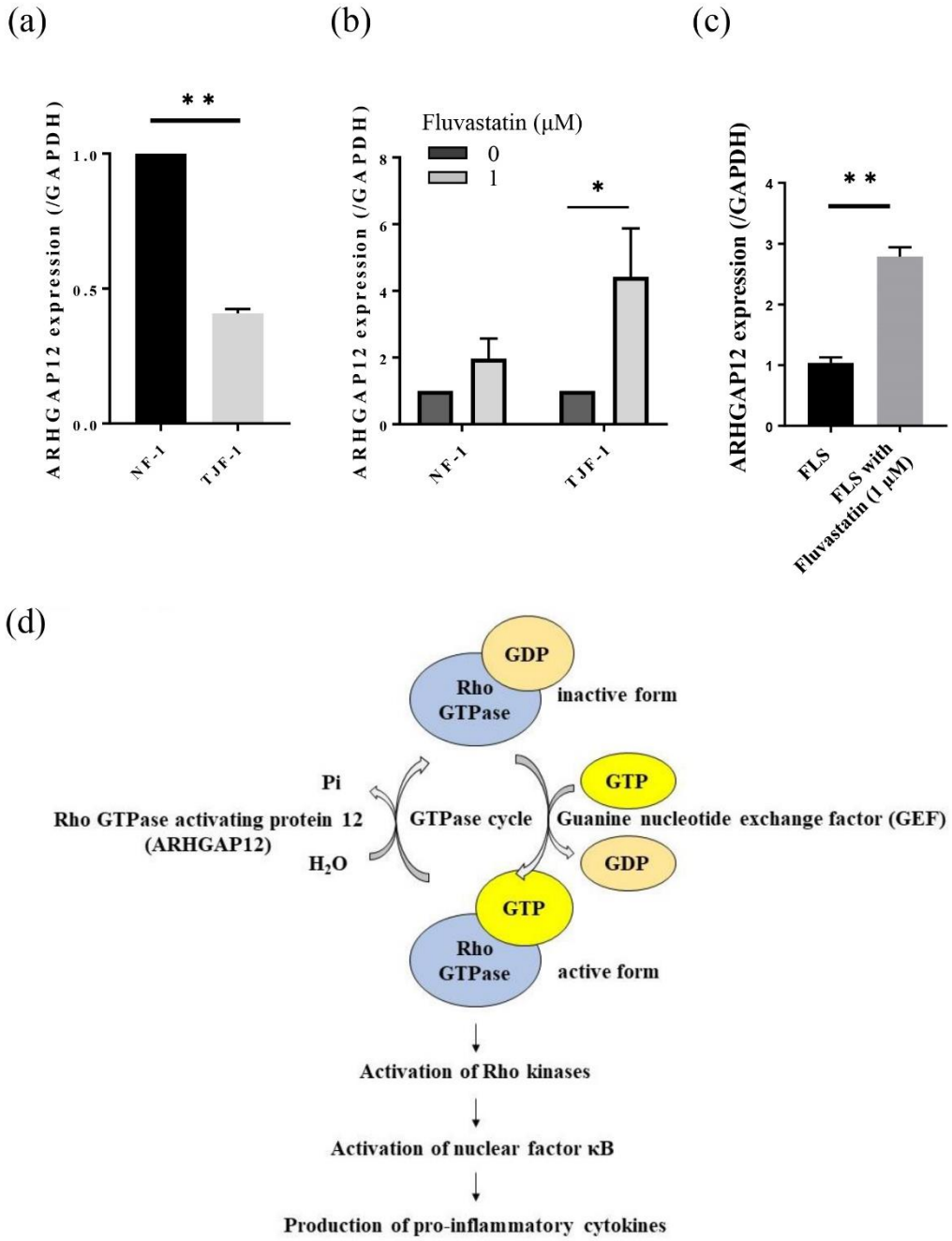

Figure 5. mRNA expression levels of *Arhgap12* in synovial fibroblasts

(**a**) Comparison of the mRNA expression levels of *Arhgap12* between NF-1, synovial fibroblasts derived from a non-arthritic wild-type rat and TJF-1, synovial fibroblasts derived from an arthritic env-pX rat. (**b**) Alteration of the mRNA expression levels of *Arhgap12* by fluvastatin (1 μM). Experiments were repeated at least three times. Data are mean±standard deviation. (**c**) Alteration of the mRNA expression levels of *Arhgap12* by fluvastatin (1 μM) in FLS, synovial fibroblasts derived from a patient with RA. Experiments were done in triplicate. Data are mean±SE. **p*<0.05, ***p*<0.01 (Student's *t*-test). (**d**) The role of ARHGAP12 in the GTPase cycle.

Table 1. Effect of fluvastatin on RF

Rats		Day 0	Day 10	Day 20	Day 30
Group 1 (Fluvastatin)	No. 1	0	0	0	0
	No. 2	0	0	0	0
	No. 3	0	0	×80	×160
	No. 4	0	0	0	0
	No. 5	0	0	0	0
Group 2 (Control)	No. 1	0	0	0	0
	No. 2	0	0	×80	×1280
	No. 3	0	0	×80	×640
	No. 4	0	0	×640	×640

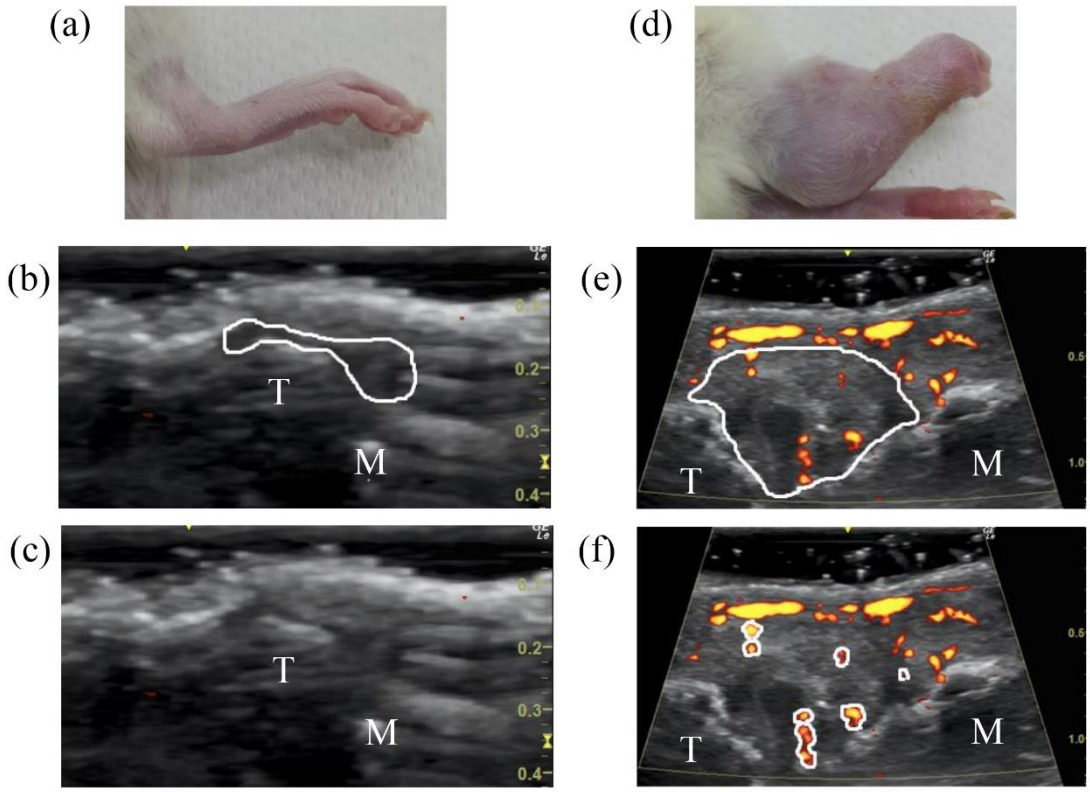

Figure S1. Macroscopic and US images of the rat ankle joints

Photographs of the rat ankle joints (**a** and **d**) and US images with PD (**b**, **c**, **e**, and **f**). (**a**–**c)** Images of the same ankle joint without swelling. (**d**–**f)** Images of the same ankle joint with swelling. T, tibia; M, metatarsal bone. White lines in **b** and **e** represent the ROI that displays the synovium. White lines in **f** display the PD signals in the synovium. No PD signal in **b** and **c**.

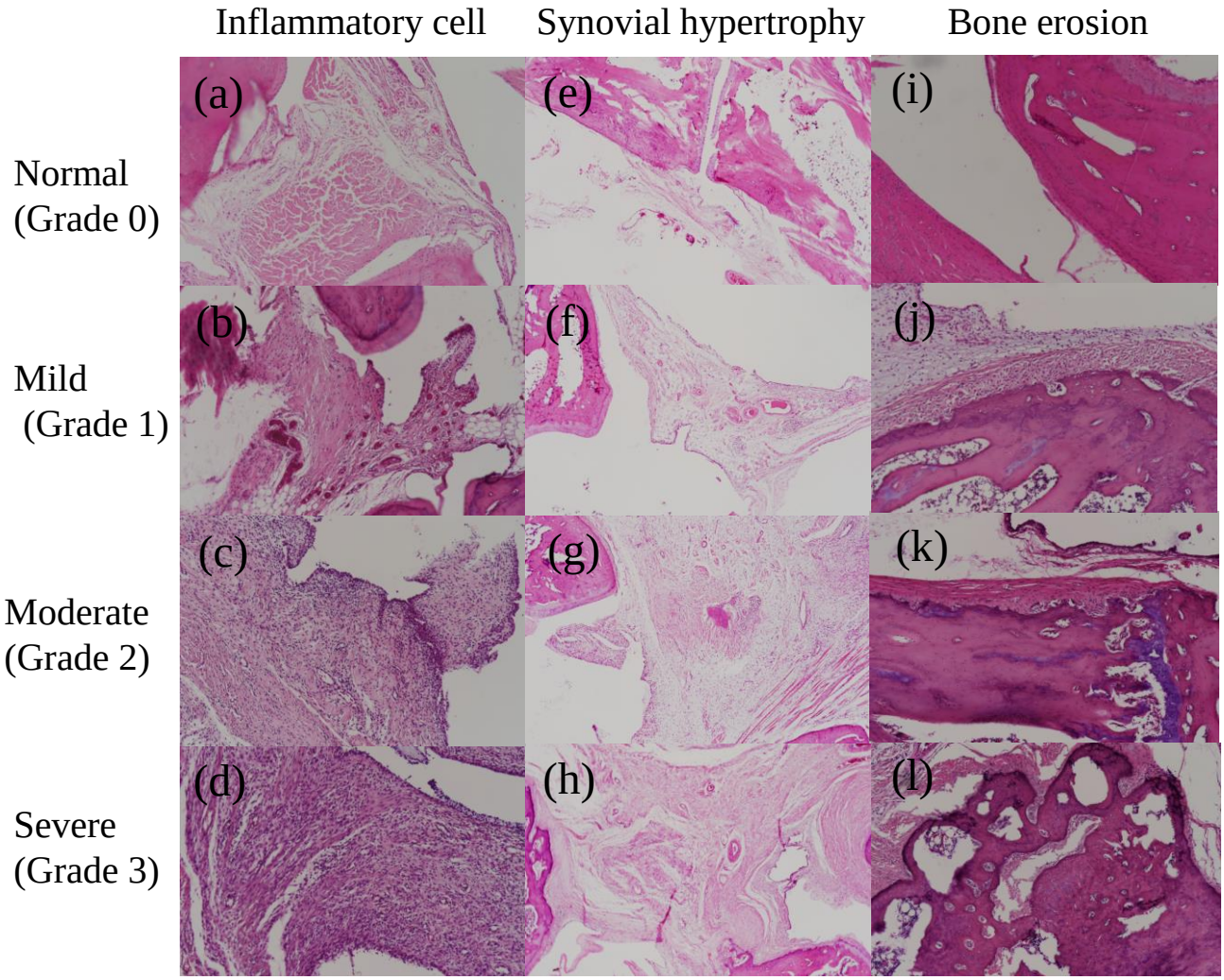

Figure S2. Histological grading scores of RA

Histological scores of RA based on the grading of periarticular inflammation (infiltration of mononuclear cells), synovial hypertrophy (pannus formation), and subchondral bone erosion. Representative findings are shown. The grade ranges 0 to 3: 0 as normal (**a**, **e**, and **i**), 1 as mild (**b**, **f**, and **j**), 2 as moderate (**c**, **g**, and **k**), and 3 as severe (**d**, **h**, and **l**).

Table S1. Primers for rat and human genes

Genes	Forward (5′-3′)	Reverse (5′-3′)
Rat Arhgap12	GGGACCTCATTTGCTGCTTT	TCGGCACTTAAGACTGCCAC
Rat Gapdh	AACGGCACAGTCAAGGCTGA	ACGCCAGTAGACTCCACGACAT
Human Arhgap12	TGGTTTGGATATTGATGGGATATACA	CATTCAAGTCCAATTTCTCATCATG
Human Gapdh	TGACAACTTTGGTATCGTGGAAGG	AGGCAGGGATGATGTTCTGGAGAG

Table S2. Serum exosomal miRNAs with more than twice the difference between Groups 1 and 2

miRNA	Target score	Target gene symbol	Target gene description
6215	99	*Plagl1*	*pleiomorphic adenoma gene-like 1*
	98	*Tmem35*	*transmembrane protein 35*
	94	*Cpsf6*	*cleavage and polyadenylation specific factor 6, 68 kDa*
	94	*Strn3*	*striatin, calmodulin binding protein 3*
17-5p	100	*Atg16l1*	*autophagy related 16-like 1 (*Saccharomyces cerevisiae*)*
	100	*Ptpn4*	*protein tyrosine phosphatase, non-receptor type 4*
	100	*Zfyve9*	*zinc finger, FYVE domain containing 9*
	100	*Epha4*	*Eph receptor A4*
	100	*Arhgap12*	*Rho GTPase-activating protein 12*
20a-5p	100	*Arhgap12*	*Rho GTPase-activating protein 12*
	100	*Ptpn4*	*protein tyrosine phosphatase, non-receptor type 4*
	100	*Atg16l1*	*autophagy-related 16-like 1 (*S. cerevisiae*)*
	100	*Epha4*	*protein tyrosine phosphatase, non-receptor type 4*
	100	*Tnfrst21*	*tumor necrosis factor receptor superfamily, member 21*
	100	*Zfyve9*	*zinc finger, FYVE domain containing 9*
20b-5p	100	*Tnfrst21*	*tumor necrosis factor receptor superfamily, member 21*
	100	*Arhgap12*	*Rho GTPase-activating protein 12*
	100	*Ptpn4*	*protein tyrosine phosphatase, non-receptor type 4*
	100	*Epha4*	*Eph receptor A4*
	100	*Zfyve9*	*zinc finger, FYVE domain containing 9*

665	100	*Syn1*	*synapsin I*
352	98	*Api5*	*apoptosis inhibitor 5*
	95	*Igf2r*	*insulin-like growth factor 2 receptor*
	94	*Ankrd17*	*ankyrin repeat domain 17*
26a-5p	100	*Chic1*	*cysteine-rich hydrophobic domain 1*
	100	*UlK2*	*unc-51-like autophagy activating kinase 2*
1224	99	*Mdh1b*	*malate dehydrogenase 1B, NAD (soluble)*
	97	*Fam211a*	*family with sequence similarity 211, member A*
	96	*Cdip1*	*cell death-inducing p53 target 1*
25-5p	90	*Prrt1*	*proline-rich transmembrane protein 1*
203a-3p	100	*Fam84a*	*family with sequence similarity 84, member A*
	100	*Mef2c*	*myocyte enhancer factor 2C*
	99	*Ell2*	*elongation factor RNA polymerase II 2*
	99	*Gabarapl1*	*GABA(A) receptor-associated protein like 1*